Vascular endothelial growth factor B regulates insulin secretion in β cells of type 2 diabetes mellitus mice via PLCγ and the IP3R-evoked Ca^{2+}/CaMK2 signaling pathway

YUQI LI[1*], RONGRONG LI[1*], XU LUO[1,2], FANG XU[1], MEIZI YANG[3], LANHUI ZHENG[4], QIHAO WU[4], WENGUO JIANG[5] and YANA LI[1]

[1]Department of Pathophysiology, School of Basic Medicine of Binzhou Medical University, Yantai, Shandong 264000; [2]Department of Laboratory, Guiyang Centers for Disease Control and Prevention, Guiyang, Guizhou 550000; [3]Department of Pharmacology, School of Basic Medicine of Binzhou Medical University, Yantai; [4]The First School of Clinical Medicine; [5]Department of Pharmacy, Binzhou Medical University, Yantai, Shandong 264000, P.R. China

Received March 1, 2023; Accepted August 9, 2023

DOI: 10.3892/mmr.2023.13084

Abstract. Vascular endothelial growth factor B (VEGFB) plays a crucial role in glucolipid metabolism and is highly associated with type 2 diabetes mellitus (T2DM). The role of VEGFB in the insulin secretion of β cells remains unverified. Thus, the present study aimed to discuss the effect of VEGFB on regulating insulin secretion in T2DM development, and its underlying mechanism. A high-fat diet and streptozocin (STZ) were used for inducing T2DM in mice model, and VEGFB gene in islet cells of T2DM mice was knocked out by CRISPR Cas9 and overexpressed by adeno-Associated Virus (AAV) injection. The effect of VEGFB and its underlying mechanism was assessed by light microscopy, electron microscopy and fluorescence confocal microscopy, enzyme-linked immunosorbent assay, mass spectrometer and western blot analysis. The decrement of insulin secretion in islet β cell of T2DM mice were aggravated and blood glucose remained at a high level after VEGFB knockout (KO). However, glucose tolerance and insulin sensitivity of T2DM mice were improved after the AAV-$VEGFB^{186}$ injection. VEGFB KO or overexpression can inhibit or activate PLCγ/IP3R in a VEGFR1-dependent manner. Then, the change of PLCγ/IP3R caused by VEGFB/VEGFR1 will alter the expression of key factors on the Ca^{2+}/CaMK2 signaling pathway such as PPP3CA. Moreover, VEGFB can cause altered insulin secretion by changing the calcium concentration in β cells of T2DM mice. These findings indicated that VEGFB activated the Ca^{2+}/CaMK2 pathway via VEGFR1-PLCγ and IP3R pathway to regulate insulin secretion, which provides new insight into the regulatory mechanism of abnormal insulin secretion in T2DM.

Correspondence to: Professor Wenguo Jiang, Department of Pharmacy, Binzhou Medical University, 346 Guanhai Road, Yantai, Shandong 264000, P.R. China
E-mail: jiangwg@bzmc.edu.cn

Professor Yana Li, Department of Pathophysiology, School of Basic Medicine of Binzhou Medical University, 346 Guanhai Road, Yantai, Shandong 264000, P.R. China
E-mail: yaya-698@163.com

*Contributed equally

Key words: VEGFB, insulin secretion, β cell, type 2 diabetes mellitus, PLCγ/IP3R, Ca^{2+}/CaMK2

Introduction

Diabetes is a metabolic disease characterized by chronic hyperglycemia caused by multiple etiologies, which is caused by defects in insulin secretion and/or utilization (1). Insulin secretion and its regulation play an important role in glucose metabolism and homeostasis (2). The abnormal and incontrollable insulin secretion in β cells is closely related to the occurrence of diabetes, but its molecular mechanism has not been fully understood and remains need to be further clarified. In recent years, the role of VEGFB in regulating lipid and glucose metabolism has attracted extensive attention. The present study found that VEGFB is related to total cholesterol (TC), triglyceride (TG), and glycosylated hemoglobin (GHb) in T2DM patients (3). In type 2 diabetes mellitus (T2DM) mice, systemic inhibition of VEGFB improves glucose tolerance and insulin sensitivity (4). Specific VEGFB overexpression in rats can ameliorate diabetes by improving insulin action (5). Targeted overexpression of the VEGFB signal can improve some key factors that promote the development of T2DM, including glucose tolerance, abnormal lipid metabolism and β cell function. Therefore, VEGFB may become an important regulatory approach in the development of T2DM.

Insulin secretion is a complex process, and calcium channels on β cell membrane play an important regulatory role during this process (6). The change in intracellular Ca^{2+} concentration is closely related to insulin secretion (7). Previous studies have shown that abnormal insulin secretion in patients with

diabetes may be related to the dysfunction of the intracellular calcium signaling pathway (8). At present and to the best of the authors' knowledge, the pathophysiological mechanism of abnormal insulin secretion remains unclear. Although it has been revealed that VEGFB can regulate insulin secretion by affecting fatty acid content, its specific regulatory mechanism also needs to be studied in the future. VEGFB transduces signals through the protein kinase C pathway (9). Therefore, can VEGFB stimulate the release of Ca^{2+} through phosphatidylinositol 3-kinase, phospholipase C-1, GTPase activating protein, and other signal proteins after it combines with VEGFR1. The answer to these scientific questions will help to further analyze the pathogenesis of diabetes and provide a theoretical basis for the precise treatment for it.

The potential molecular mechanism of abnormal insulin secretion in β cells of T2DM mice were examined. VEGFB knockout (KO) or overexpression can inhibit or activate phospholipase C gamma (PLCγ) and inositol 1,4,5-triphosphate receptor IP3R signaling pathway in a VEGFR1-dependent way. Then, the change of PLCγ/IP3R caused by VEGFB/VEGFR1 will alter the expression of key factors on the calcium/calmodulin signaling pathways such as PPP3CA. KO or overexpression of VEGFB can cause altered insulin secretion by changing the calcium concentration in β cells and affect the glucose tolerance and insulin sensitivity of T2DM mice. The present study demonstrated that VEGFB can regulate insulin secretion via PLCγ and the IP3R-evoked Ca^{2+}/CaMK2 signaling pathway.

Materials and methods

Experimental animals. The experiments on mice were approved (IACUC approval no: 2022-210) by the animal ethics committee of Binzhou Medical University (Yantai, China). All mice were raised at 24˚C, 12/12-h light/dark, 50% humidity). C57BL/6 male mice (n=6) (age, 4 weeks-old; weight, 16-18 g), were selected into 5 experimental groups: wild-type (WT), streptozocin (STZ)-WT, STZ-KO, adeno-associated virus (AAV)-control, and AAV-$VEGFB^{186}$ group. $VEGFB^{+/+}$ mice fed standard diet (SD, Rodent Diet with 10% kcal% fat, Jiangsu Xietong Pharmaceutical Bio-engineering Co., Ltd.) were named the WT group (n=6). A total of four groups of mice induced by STZ and high-fat diet (HFD, Rodent Diet with 60% kcal% fat, Research Diets, Inc.) were T2DM models. WT group was not induced with STZ. $VEGFB^{+/+}$ T2DM mice were named STZ-WT (n=6), and $VEGFB^{-/-}$ T2DM mice were named STZ-KO (n=6). $VEGFB^{+/+}$ T2DM mice injected with AAV targeting $VEGFB^{186}$ were named the AAV-$VEGFB^{186}$ group (n=6), and mice in the AAV-control group were injected with non-targeting $VEGFB^{186}$ and were regarded as the negative control (n=6). WT, STZ-WT and STZ-KO groups of mice were euthanized and measured in the 24th week. Some mice developed complications of T2DM after 32 weeks due to the longer course of T2DM, therefore the latter two groups were in the 32nd week (10-13). In the animal experiment, all mice were administered 3% isoflurane, and sacrificed by cervical dislocation after blood collection from the eyeball. Pancreatic tissues of mice were removed and fixed with 4% paraformaldehyde or 2.5% glutaraldehyde.

Cell culture and treatment. Mouse islet β cell line Min6 was purchased from the Procell Life Science&Technology Company and was cultured in RPMI-1640 (Gibco; Thermo Fisher Scientific, Inc.) medium containing 10% fetal bovine serum, and 1% Penicillin/streptomycin (P/S). The temperature inside the incubator was 37˚C and the gas proportion was 5% CO_2. Min6 cells were adhered in the six-well plate to the confluence of 50% and grouped into negative control (NC) and silencing (SI) groups. Cells in the NC group were treated with non-targeting VEGFB sequence (5'UUCUCCGAACGU GUCACGUTT3', 3' ACGUGACACGUUCGGAGAATT 5') while SI groups were treated with VEGFB KO sequence [VEGFB small interfering RNA (siRNA): 5'GAACACAGC CAATGTGAAT 3'] in the SI group. JetPRIME and Jet buffer (Polyplus-transfection® Inc., United States) were used to transfect the sequence within 48 h at room temperature and then the cells in two groups were detected the efficiency of transfection by reverse transcription-quantitative (RT-q) PCR and western blot analysis.

VEGFB KO mouse. VEGFB KO mouse model was constructed by CRISPR/Cas 9 technology. The work was undertaken by the Saiye (Guangzhou) Biotechnology Co., Ltd. The gRNA sequences were as follows: gRNA-1, 5'-AAGGGCTCCGTC CTTGAGTCAGG-3'; and gRNA-2, 5'-CAGGGGATGACT TATGGGCCAGG-3'. The wild-type mice were not transfected with any control construct. A total of two pairs of primers were used for the PCR cycle and the sequences were as follows: primer 1 forward, 5'-TCTCAAGGTTGGCGGAAGTGG-3' and reverse, 5'-CAAACTCACCATGTCACCAAGGAG-3'; and primer 2 forward, 5'-TCTCAAGGTTGGCGGAAG TGG-3' and reverse, 5'-TTGGGATCACGCAAGATAAGG G-3'. Mice genotypes were identified by 12% agarose gel electrophoresis and visualized by ethidium bromide, $VEGFB^{+/+}$ and $VEGFB^{-/-}$ mice were screened for the T2DM model. In the present study, the protein and mRNA levels of VEGFB expression in $VEGFB^{+/+}$ and $VEGFB^{-/-}$ mice were detected in the pancreas (Fig. 1A-D).

T2DM mouse model. The mice were fed with HFD from the 8th week. STZ was intraperitoneally injected twice at a dose of 30 mg/kg within the 15-16th weeks, with an interval of 1 day between the two injections (14,15). The blood glucose of mice was measured at 0, 3, 10 and 30 days after injection of STZ. Four weeks after STZ injection, the mice with fasting blood glucose (FBG) ≥11.1 mmol/l were defined as the T2DM model (Fig. 1E).

Overexpression of VEGFB in T2DM mouse. The AAV vector was purchased from the OBiO Technology (Shanghai) Corp., Ltd. AAV-CAG-$VEGFB^{186}$-P2A-EGFP-3xFLAG-WPRE was regarded as an overexpression vector and AAV-CAG-EGFP-3xFLAG-WPRE was a control vector. A total of eight weeks after injection with STZ, the mice whose FBG was ≥16.7 mmol/l were prepared for intraperitoneal AAV infection into the pancreas. The virus titer was controlled $>1.0x10^{12}$ on each side (Fig. 1F-I).

Measurement of weight, FBG and postprandial blood glucose (PBG). From the 8th week, the three indicators were measured at a fixed time every week. The mice were not fed within 12 h and FBG was examined. After the mice were administered

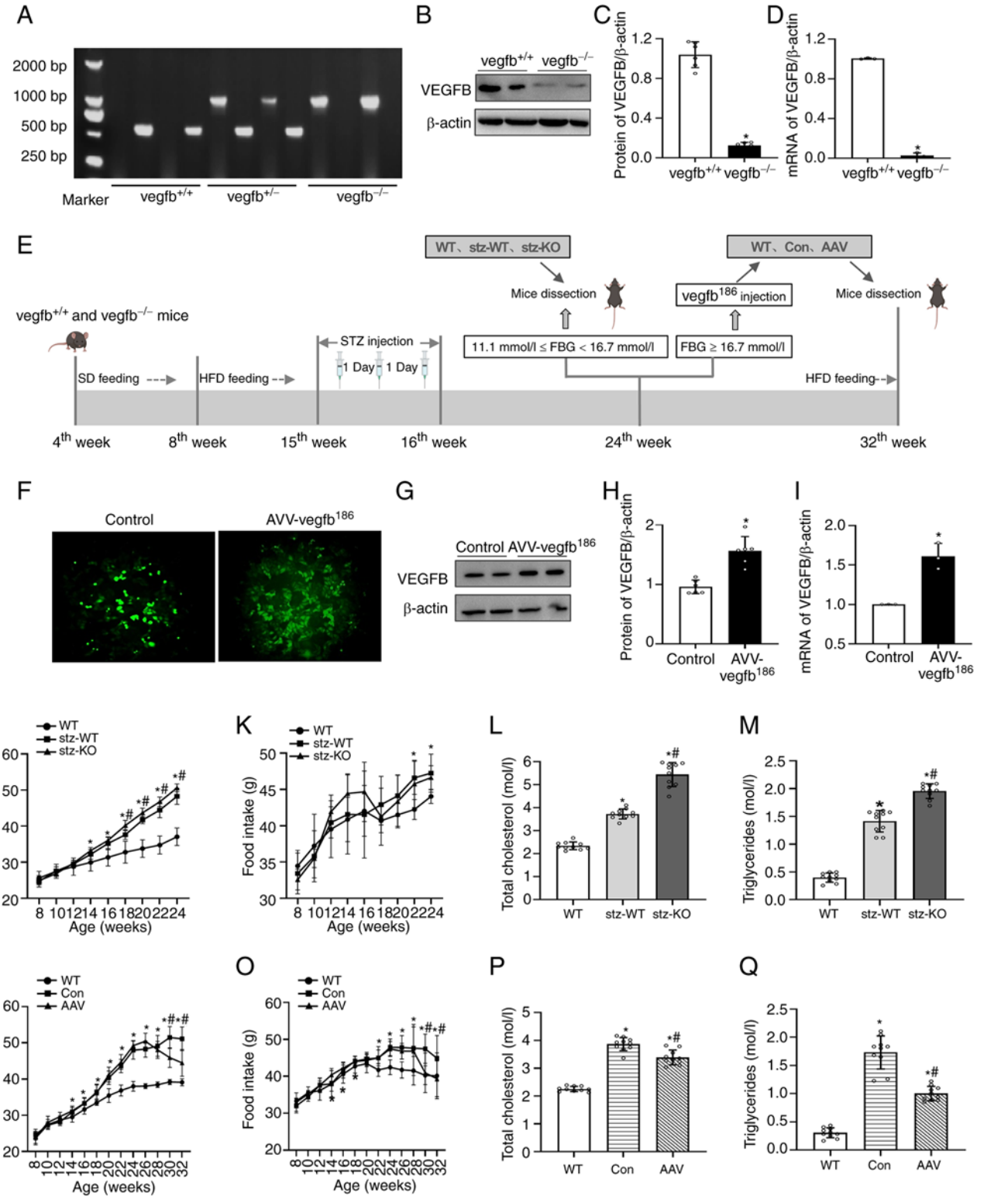

Figure 1. Construction of the experimental animal model and the effect of VEGFB on food and body weight. (A) Gene identification of VEGFB knockout mice. (B and C) The protein expression of VEGFB in mice (n=6). (D) The mRNA expression of VEGFB in mice (n=3). (E) The flow diagram of animal experiment design. (F) Fluorescent expression of AAV-control and AAV-VEGFB^{186} in T2DM mice. (G and H) The protein expression of VEGFB in T2DM mice (n=6). (I) mRNA expression of VEGFB in mice (n=3). (J and K) Body weight and food intake of WT, STZ-WT, and STZ-KO mice (n=9). (L and M) TC and TG content of WT, STZ-WT, and STZ-KO mice (n=10). *P<0.05 vs. WT; $^{\#}$P<0.05 vs. STZ-WT. (N and O) Body weight and food intake of WT, AAV-control and AAV-VEGFB^{186} mice (n=9). (P and Q) TC and TG content of WT, AAV-control and AAV-VEGFB^{186} mice (n=10). *P<0.05 vs. WT; $^{\#}$P<0.05 vs. AAV-control. VEGFB, vascular endothelial growth factor B; AAV, adeno-associated virus; T2DM, type 2 diabetes mellitus; WT, wild-type; STZ, streptozocin; KO, knockout; TC, total cholesterol; TG, triglyceride.

a resumption of diet for 2 h, the PBG was measured. The blood was drawn from the tail vein by using a Roche blood glucose meter (Roche Diabetes Care, Inc.) for FBG and PBG measurement.

Table I. List of primary antibodies used.

Primary antibody	Dilution ratio	Source	Cat. no.	Supplier
PPP3CA	1:1,000	Rabbit	DF6208	Affinity
PLCγ	1:1,000	Rabbit	AF6210	Affinity
IP3R	1:1,000	Rabbit	DF3000	Affinity
CAMK2	1:1,000	Rabbit	AF6493	Affinity
VEGFR1	1:1,000	Rabbit	AF6204	Affinity
VEGFB	1:1,000	Rabbit	AF7019	Affinity
β-actin	1:1,000	Mouse	T0022	Affinity

VEGFB, vascular endothelial growth factor B.

Isolation of islet cells. A total of three mice in each group were used to isolate islets, and 100-150 islet cell clusters could be collected from each mouse. The pancreas was removed, and the peripheral adipose tissue was isolated and placed in Hank's buffer after the mice's death. Collagenase P (0.5 mg/ml; Roche) was injected through the pancreatic duct and digested for 10 min after complete expansion of the pancreas. Hank's buffer was pre-cooled at 4˚C to stop digestion, and cell mass was selected under the stereoscopic microscope (Olympus Corporation).

Western blot analysis. Lysates consisting of 1% cocktail RIPA (cat. no. R0010; Beijing Solarbio Science & Technology Co., Ltd.) and PMSF (cat. no. 36978; Gibco; Thermo Fisher Scientific, Inc.) were added to the cells from islet cell clusters on ice for 30 min. The loading buffer (cat. no. D1020-5; Beijing Solarbio Science & Technology Co., Ltd.) was added to the supernatant and heated after centrifugation. Protein samples (20 μg protein /lane) were transferred onto PVDF membranes after separating in 10% SDS-PAGE gel. After blocking with 5% skimmed milk at room temperature for 1 h, membranes were incubated with primary antibodies at 4˚C (Table I). After 12 h, membranes were incubated with secondary antibodies (1:5,000, cat. no. S0001, Affinity, HRP) at room temperature for 2 h. Optical density was detected after samples were treated with enhanced chemiluminescence reaction (Tanon 5200; Tanon Science & Technology Co., Ltd.). The blots were performed densitometric analysis by ImageJ software (version 1.52a, National Institutes of Health)

RT-qPCR. Total RNA was collected from islet cell clusters with TriQuick Reagent (cat. no. R100; Beijing Solarbio Science & Technology Co., Ltd.). RNA-easy Isolation Reagent (Vazyme Biotech Co., Ltd.) reverse transcription and real-time detection were accomplished with TB Green Premix Ex Taq II (Takara Bio, Inc.) fluorescence quantitative kit on PCR QuantStudio 3 (Thermo Fisher Scientific, Inc.). The thermo cycling conditions of RT-qPCR were as follows: Initial denaturation at 95˚C for 30 sec; then 40 cycles were conducted at 95˚C for 5 sec and 60˚C for 34 sec; the dissolution process was performed at 95˚C, 60˚C and 95˚C for 15 sec, 1 min and 15 sec, respectively in the end. The primer sequences were as follows: VEGFB forward, 5'-GCTGGGCACTAGTTGTTTG-3' and reverse, 5'-AGCCACCAGAAGAAAGTGG-3'; and β-actin forward, 5'-CATCCGTAAAGACCTCTATGCCAAC-3' and reverse, 5'-ATGGAGCCACCGATCCACA-3'. The $2^{-\Delta\Delta Cq}$ method was used to quantify the expression of mRNA by using β-actin as an internal reference gene (16).

ELISA and colorimetry. Serums from five mice were collected for measurement of blood glucose (cat. no. ml016964), GHb (cat. no. ml063816) and insulin (cat. no. ml001983) content with a microplate reader (BioTek Corp.) by ELISA. A standard curve was established according to the measured value of the standard and the sample content was calculated. TG (cat. no. A110-1-1), and TC (cat. no. A111-1-1; both from Nanjing Jiancheng Bioengineering Institute) were detected by the colorimetry method according to the manufacturer's instructions.

Hematoxylin and eosin (H&E) Staining. Pancreatic tissues of 3 mice in each group were fixed with 4% paraformaldehyde at 4˚C for 12 h. After dehydration by an automatic dehydrator, tissue was embedded with paraffin, and sliced into 5-μm sections. The section was dewaxed to water with xylene and stained with hematoxylin for 5 min and eosin for 1 min at room temperature. After sealing with neutral glue, the images of the samples were acquired by the optical microscope (OLYMPUS-DP27; Olympus Corporation).

Transmission electron microscopy. The pancreas tissues of 3 mice in each group were fixed with 2.5% glutaraldehyde solution and 1% osmic acid at 4˚C for 12 h. Tissues were subjected to mixed treatment with entrapment agent and acetone (v/v=1/2) after dehydration with gradient alcohol, pure entrapment agent-permeated and embedded. Subsequently, they were sliced with Reichert ultra-thin microtome (70 nm). Lead citrate solution and uranyl acetate 50% ethanol saturated solution were used for staining at room temperature for 10 min, respectively. A transmission electron microscope (JEM-1400; JEOL, Ltd.) was used to observe and capture images of the sections.

Immunofluorescence. After paraffin removal with xylene, gradient hydration with ethanol and antigen repair with sodium citrate and 3% H_2O_2 solution-eliminated endogenous peroxidase activity, 5% goat serum (cat. no. SL038, Solarbio) was used for blocking at 37˚C for 30 min. Then the antibody mixture of insulin (1:200; cat. no. 66198-1-ig; ProteinTech

Group, Inc.) and glucagon (1:100; cat. no. ab92517; Abcam) was added dropwise and incubated for 12 h in a 4˚C wet box. The next day, the mixture of fluorescent goat anti-rabbit IgG/TRITC (1:100; cat. no. ZF-0317; OriGene Technologies, Inc.) and goat anti-mouse IgG/FITC (1:100; cat. no. ZF-0314; OriGene Technologies, Inc.) was added and incubated for 1 h. Afterwards, it was stained with 10 μg/ml DAPI, rinsed, blocked, and stored at 4˚C without light after washing with PBS. Images were captured by a confocal laser scanning microscope (LSM880; Zeiss AG).

Oral glucose tolerance test (OGTT) and intraperitoneal insulin tolerance test (IPITT). During the OGTT, mice were not fed within 12 h and then ravaged with 40% glucose at the dose of 2 mg/kg. During the IPITT, the mice were injected intraperitoneally with 0.5 UI/kg insulin after fasting for 6 h. Blood glucose at 0, 15, 30, 60, 90 and 120 min was detected.

Islet secretion function index. FBG, fasting insulin (FINS), insulin increment (ΔI30), and glucose increment (ΔG30) at 30 min in OGTT, 1 and 2 h of PBG of five mice in each group were detected. Insulin secretion index of the steady-state model (HOMA-β)=FINS x20/(FBG-3.5); Islet β cells secretion index (ΔI30/ΔG30)=the ratio of insulin increment to glucose increment in OGTT at 30 min; modified β cells function index=(FINS x FBG)/(PBG 1 h + PBG 2h-2FBG).

Glucose stimulation. Min6 cell line and islet cells from 3 mice in each group were used for the detection. Fresh islets and Min6 cells were cultured overnight in the sugar-free medium at 37˚C. After washing, they were cultured with 2.8 mmol/l low-sugar medium at 37˚C for 2 h, and incubation medium was collected to detect insulin (Shanghai Enzyme-linked Biotechnology Co., Ltd.; cat. no. ml001983) and intracellular Ca^{2+} content (Shanghai Enzyme-linked Biotechnology Co., Ltd.; cat. no. ml058009). And then 16.7 mmol/l high-sugar medium was replaced for the incubation.

Calcium content analyses. Intracellular calcium content was detected according to the manufacturer's instructions (cat. no. ml058009). Diluted standard and samples were added to the 96-well plate with 50 μl, and then the antibodies were added with 50 μl. The membrane plate was covered, gently shaken and mixed, and incubated at 37˚C for 1 h. The enzyme HRP was added after washing with buffer three times and incubated at 37˚C for 30 min. A total of 50 μl of substrates A and B was added to each well, gently shaken and mixed, and incubated at 37˚C for 10 min without light. The OD value was measured at a wavelength of 450 nm after adding 50 μl of termination solution.

Proteomic analysis. Islet cells of five $VEGFB^{+/+}$ and $VEGFB^{-/-}$ mice were isolated. Meanwhile, islet cells of five $VEGFB^{+/+STZ}$ and $VEGFB^{-/-STZ}$ mice were isolated for proteomic analysis. PBS containing protease inhibitors and phosphatase inhibitors were used to treat cells. And then homogenated in a denatured buffer containing urea, HEPES. The Bradford assay (Bio-Rad Laboratories, Inc.) was used to examine the protein content. DL-Dithiothreitol solution and Iodoacetic amide solution were added. Trypsin/Lys-C (FUJIFILM Wako Pure Chemical Corporation) was added so that the final concentration of the sample digestion buffer was 5% (w/w) trypsin/protein. Trifluoroacetic acid and acetonitrile (ACN) were used for column washing. The peptide elution fractions were labeled with 6-plex TMT reagent and then the labeled peptide was acidified with formic acid (pH 2.5), and the sample was filtered and desalted through C18 Stage-tips, and completely dried in a vacuum centrifuge. Peptides were dissolved and separated by RPLC-MS using the EASY-nLC 1000 system (Thermo Fisher Scientific, Inc.). The peptide was washed at 250 l/min with ACN concentrated from 4-100%. All results of data were analyzed by using a QExactive plus Orbitrap mass spectrometer (Thermo Fisher Scientific, Inc.). The mass spectrometer was operated in the positive ion module to obtain the investigation mass spectrum with 7000 resolution and the successive high collision dissociation fragmentation spectrum. The bioinformatics tools used to analyze the heatmap were HIPLOT (hiplot.com.cn/home/index.html) and Gene Set Analysis Toolkit (https://www.webgestalt.org).

Statistical analysis. SPSS 22.0 statistical software (IBM Corp.) was used to analyze all data. The results were shown as the mean ± SD. One-way ANOVA followed by Dunnett's post hoc test was used, while comparisons between two groups were assessed using paired Student's t-test. $P<0.05$ was considered to indicate a statistically significant difference.

Results

VEGFB regulates glucolipid metabolism and insulin sensitivity in T2DM mice. From the 14th week, the weight of mice fed HFD was higher than those of mice fed SD, and the weight of STZ-KO mice was higher in comparison with STZ-WT mice in the 18th week (Fig. 1J). There was no significant difference between SD and HFD feeding except in the 22nd and 24th week (Fig. 1K). In the 24th week, the TC and TG of STZ-KO mice were significantly higher than those of STZ-WT mice (Fig. 1L and M). When the T2DM mice were administered AAV injection, the weight and food intake of $AAV\text{-}VEGFB^{186}$ mice were decreased from the 30th week (Fig. 1N and O). And the TC and TG contents were decreased when compared with STZ mice (Fig. 1P and Q).

From the 18th week, the FBG and PBG of T2DM mice were increased. In STZ-KO mice, FBG was increased from the 22nd week and PBG was increased from the 18th week compared with STZ-WT mice (Fig. 2A and B). Under the HFD condition, the serum glucose and GHb of STZ-KO mice were higher than those of STZ-WT mice in the 24th week (Fig. 2C and D). OGTT and IPITT revealed that the ability to regulate blood glucose in T2DM mice and the efficiency of glucose uptake and utilization promoted by insulin decreased. Blood glucose of STZ-KO mice was higher than that of STZ-WT mice with the stimulation of glucose and insulin. At the same time, the area under the curve also increased (Fig. 2E-H).

Compared with the Con group, the body weight and blood glucose of mice in the AAV group decreased significantly from the 24th week, especially the decrease in PBG, indicating that VEGFB has a therapeutic effect on blood glucose in T2DM mice (Fig. 2I and J). In addition, serum glucose and GHb were

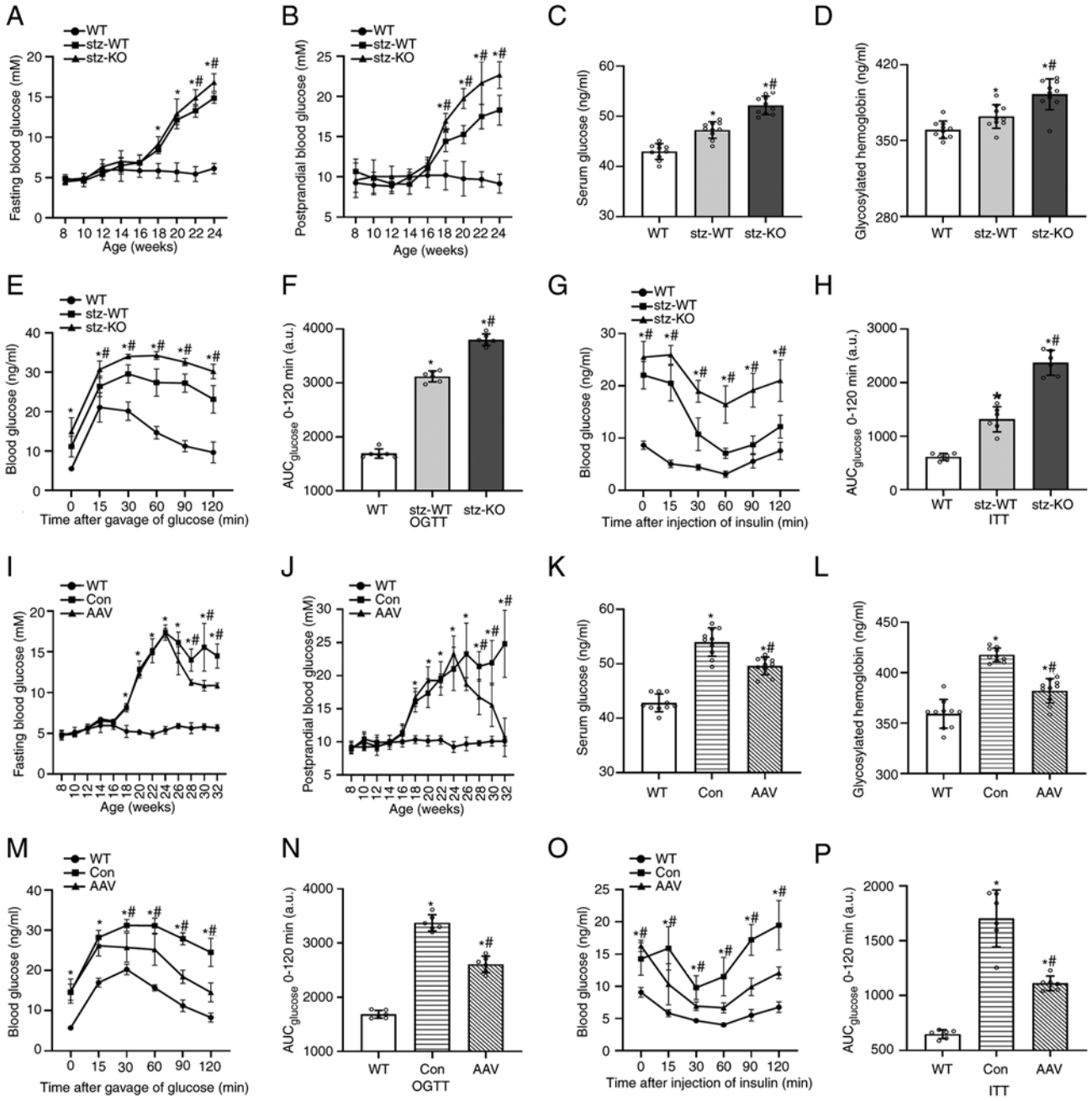

Figure 2. Effect on glucolipid metabolism in T2DM mice after VEGFB knockout and overexpression. (A and B) FBG and PBG curves of WT, STZ-WT and STZ-KO mice from the 8th to 24th weeks (n=9). (C and D) Serum glucose and GHb contents of WT, STZ-WT and STZ-KO mice (n=10). (E-H) OGTT, AUC of OGTT, IPITT, AUC of IPITT of WT, STZ-WT and STZ-KO mice (n=6). *P<0.05 vs. WT; #P<0.05 vs. STZ-WT. (I and J) FBG and PBG curves of WT, AAV-control and AAV-VEGFB^{186} mice from the 8th to 32nd weeks (n=9). (K and L) Serum glucose and GHb contents of WT, AAV-control and AAV-VEGFB^{186} mice (n=10). (M-P) OGTT, AUC of OGTT, IPITT, AUC of IPITT of WT, AAV-control and AAV-VEGFB^{186} mice (n=6). *P<0.05 vs. WT; #P<0.05 vs. AAV-control. T2DM, type 2 diabetes mellitus; VEGFB, vascular endothelial growth factor B; FBG, fasting blood glucose; PBG postprandial blood glucose; STZ, streptozocin; WT, wild-type; KO, knockout; AAV, adeno-associated virus; GHb, glycosylated hemoglobin; OGTT, oral glucose tolerance test; IPITT, intraperitoneal insulin tolerance test; AUC, area under the curve.

significantly lower in the 32nd week (Fig. 2K and L). The OGTT and ITT results demonstrated that the glucose tolerance and insulin sensitivity of AAV-VEGFB^{186} mice increased compared with the WT group but decreased compared with control group (Fig. 2M-P).

VEGFB affects insulin secretion of islet β cells in T2DM mice. Compared with WT, the serum insulin and insulin secretion function of T2DM mice was lower, while the serum insulin and insulin secretion function of the STZ-KO group was significantly lower than those of the STZ-WT group (Fig. 3A-D). After AAV injection, the serum insulin and insulin secretion function of AAV-VEGFB^{186} mice were higher than AAV-control mice (Fig. 3E-H).

The morphological changes of pancreatic islets were observed by H&E staining. It is not easy to distinguish multiple cell types in the islets under H&E staining. The endocrine cells in the islets mainly include A cells (~20% of the total islet cells),

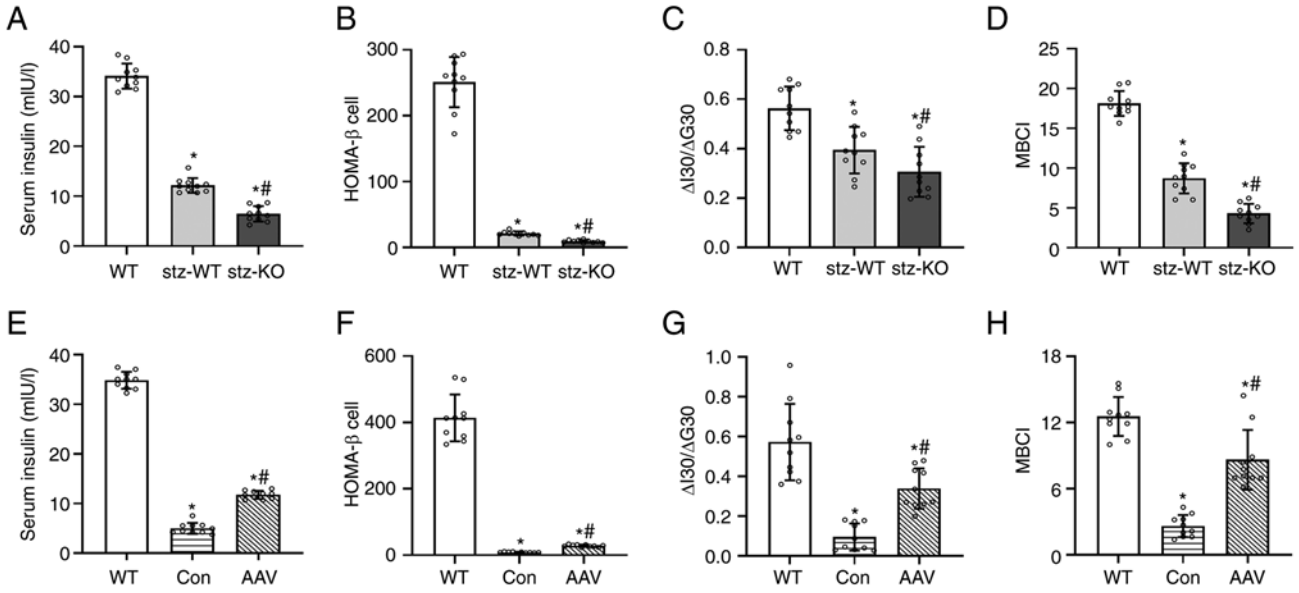

Figure 3. Effect of up- and downregulated VEGFB on serum insulin and β cell function index. (A) Serum insulin contents of WT, STZ-WT and STZ-KO mice (n=10). (B-D) HOMA-β, ΔI30/ΔG30, and MBCI of WT, STZ-WT and STZ-KO mice (n=10). *P<0.05 vs. WT; #P<0.05 vs. STZ-WT. (E) Serum insulin contents of WT, AAV-control and AAV-VEGFB^{186} mice (n=10). (F-H) HOMA-β, ΔI30/ΔG30, and MBCI of WT, AAV-control and AAV-VEGFB^{186} mice (n=10). *P<0.05 vs. WT; #P<0.05 vs. AAV-control. VEGFB, vascular endothelial growth factor B; STZ, streptozocin; WT, wild type; KO, knockout; AAV, adeno-associated virus.

B cells (~75% of the total islet cells), D cells (~5% of the total islet cells), and others such as PP cells and D1 cells (17,18). The islets of mice in the WT group were round or oval with clear boundaries and close arrangement between islet cells. The size of islets in T2DM mice was not homogeneous, and some islets showed atrophy and volume reduction. β cells, with a large number, were in the center of the islet, while α cells, with a small number, were in the periphery of the pancreas islet. The nucleus of β cells in WT was circular and intact, and secretory vesicles could also be observed. The volume of β cells and the number of mitochondria decreased in T2DM mice (Fig. 4A). After the injection of AAV-VEGFB^{186}, the size of the islet was improved (Fig. 4B).

The number of islet cells and the density of β cells in STZ-KO mice were lower than those of STZ-WT mice, and meanwhile, the density of mature and immature secretory vesicles of STZ-KO mice decreased significantly (Fig. 4C-F). Compared with AAV-control, the number of islet cells, the density of β cells, and secretory vesicles in AAV-VEGFB^{186} mice were higher (Fig. 4G-J).

VEGFB regulates insulin secretion through Ca^{2+}/CaMK2 and its association with PPP3CA. A total of 2,034 proteins were identified in the islets of VEGFB$^{+/+}$ and VEGFB$^{-/-}$ mice, of which 100 proteins were different between the two groups. A total of 34 upregulated and 12 downregulated proteins were analyzed among these differential proteins in the islets of mice (Fig. 5A). A total of 1,722 proteins were identified in the islets of STZ-WT and STZ-KO mice, of which 43 proteins were different between the two groups among these differential proteins (Fig. 5B). The heatmap showed that PPP3CA was associated with VEGFB in differential proteins (Fig. 5C). The differential proteins were analyzed by interpretative phenomenological analysis (IPA) method after VEGFB KO, which was mainly involved in cellular glucose homeostasis (Fig. 5D and E).

The protein expression of PPP3CA and CaMK2 was decreased in STZ-KO mice, while in AAV-VEGFB^{186} mice, the expression of PPP3CA and CaMK2 was increased (Fig. 5F-M). The intracellular Ca^{2+} and insulin were detected, and their contents in STZ-KO mice were lower than those of STZ-WT mice (Fig. 5N-Q), while in AAV-VEGFB^{186} mice, Ca^{2+} and insulin levels increased after glucose stimulation (Fig. 5R-U).

VEGFB/VEGFR1 affects the content of Ca^{2+} via the PLCγ/IP3R signaling pathway. In order to detect the effects of VEGFB on the PLCγ/IP3R signaling pathway, the expression of VEGFB, VEGFR1, PLCγ and IP3R was examined by western blot analysis. The results revealed that VEGFR1 protein expression was decreased as the VEGFB was knocked out, which suppressed the expression of the downstream proteins PLCγ and IP3R in STZ-KO mice (Fig. 6A-H). Moreover, the expression of VEGFR1, PLCγ and IP3R proteins were elevated in AAV-VEGFB^{186} mice with overexpressed VEGFB gene (Fig. 6I-P).

VEGFB/VEGFR1 affects the content of Ca^{2+} and insulin secretion via VEGFA in physiological state. In VEGFB$^{+/+}$ and VEGFB$^{-/-}$ mice, the serum glucose content was decreased and serum insulin was increased after the VEGFB was knocked out (Fig. S1A and B). The calcium content and insulin secretion of islet cells in VEGFB$^{-/-}$ mice significantly increased after stimulation of 2.8 and 16.7 mM glucose (Fig. S1C-F). The expression of the VEGFR1 protein declined following the loss of the VEGFB gene while the expression of VEGFA and VEGFR2 protein increased. siRNA transfection in MIN6 was performed to detect the insulin secretion and calcium content

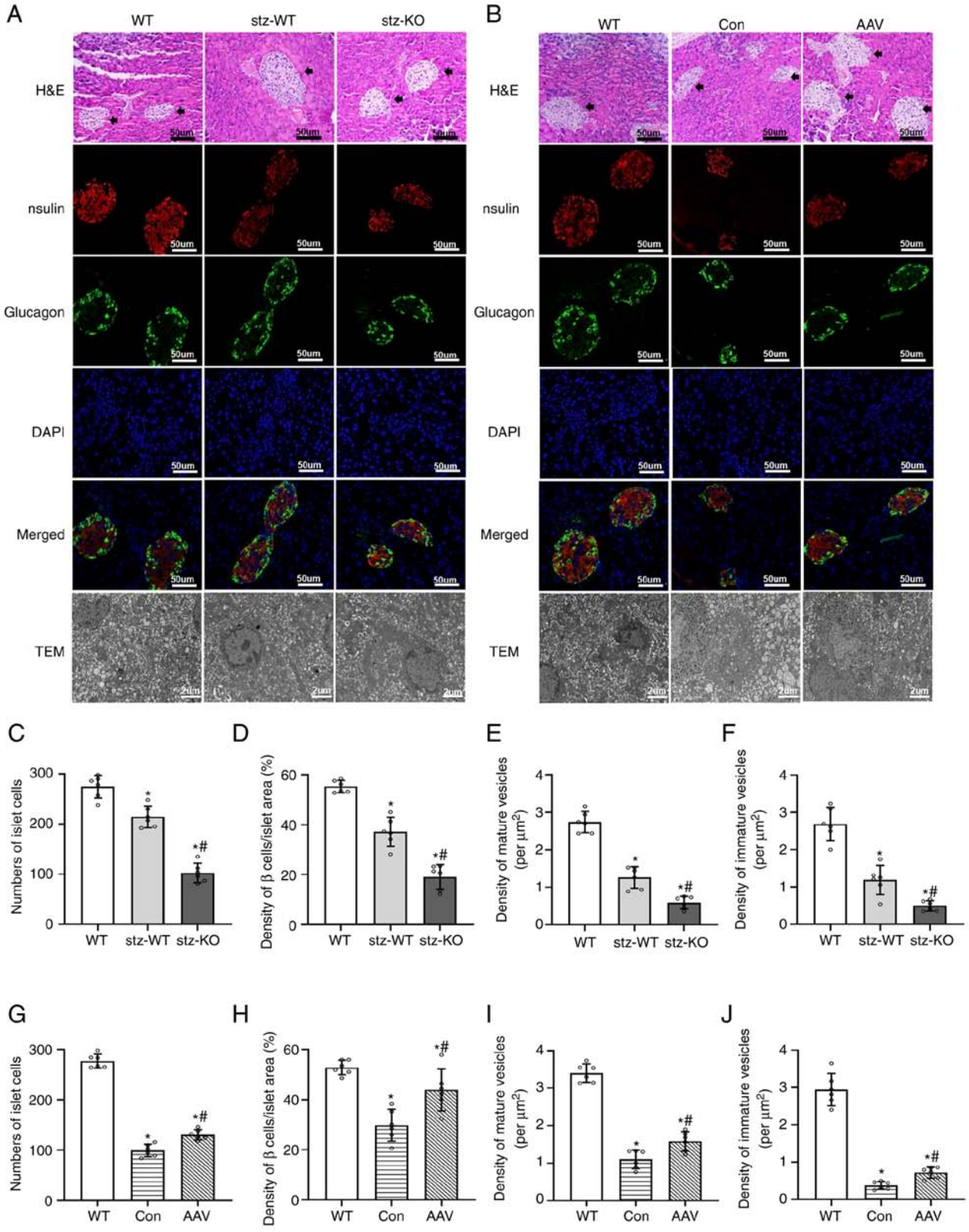

Figure 4. Effect of VEGFB on the islet, β cells and insulin secretory vesicles of mice. (A and B) The morphology of islets by light microscope (magnification, x400; scale bar, 50 μm), immunofluorescence (magnification, x400; scale bar, 50 μm), and electron microscopy (magnification, x8,000; scale bar, 2 μm). The arrows stand for the islet. (C) Number of islet cells, (D) density of β cells, and the density of (E) mature and (F) immature insulin secretory vesicles in β cells of WT, STZ-KO and STZ-WT mice (n=6). *P<0.05 vs. WT; $^{\#}$P<0.05 vs. STZ-WT. (G-J) The number of (G) islet cells, (H) the density of β cells, and the density of (I) mature and (J) immature insulin secretory vesicles in β cells of WT, AAV-control and AAV-VEGFB^{186} mice (n=6). *P<0.05 vs. WT; $^{\#}$P<0.05 vs. AAV-control. VEGFB, vascular endothelial growth factor B; STZ, streptozocin; KO, knockout; WT, wild-type; AAV, adeno-associated virus.

as the expression of VEGFB was suppressed at the protein and mRNA levels (Fig. S1J and K). The ATP, calcium and insulin secretion were increased in the SI group with the stimulation of 2.8 and 16.7 mM glucose (Fig. S1L-Q). The expression of

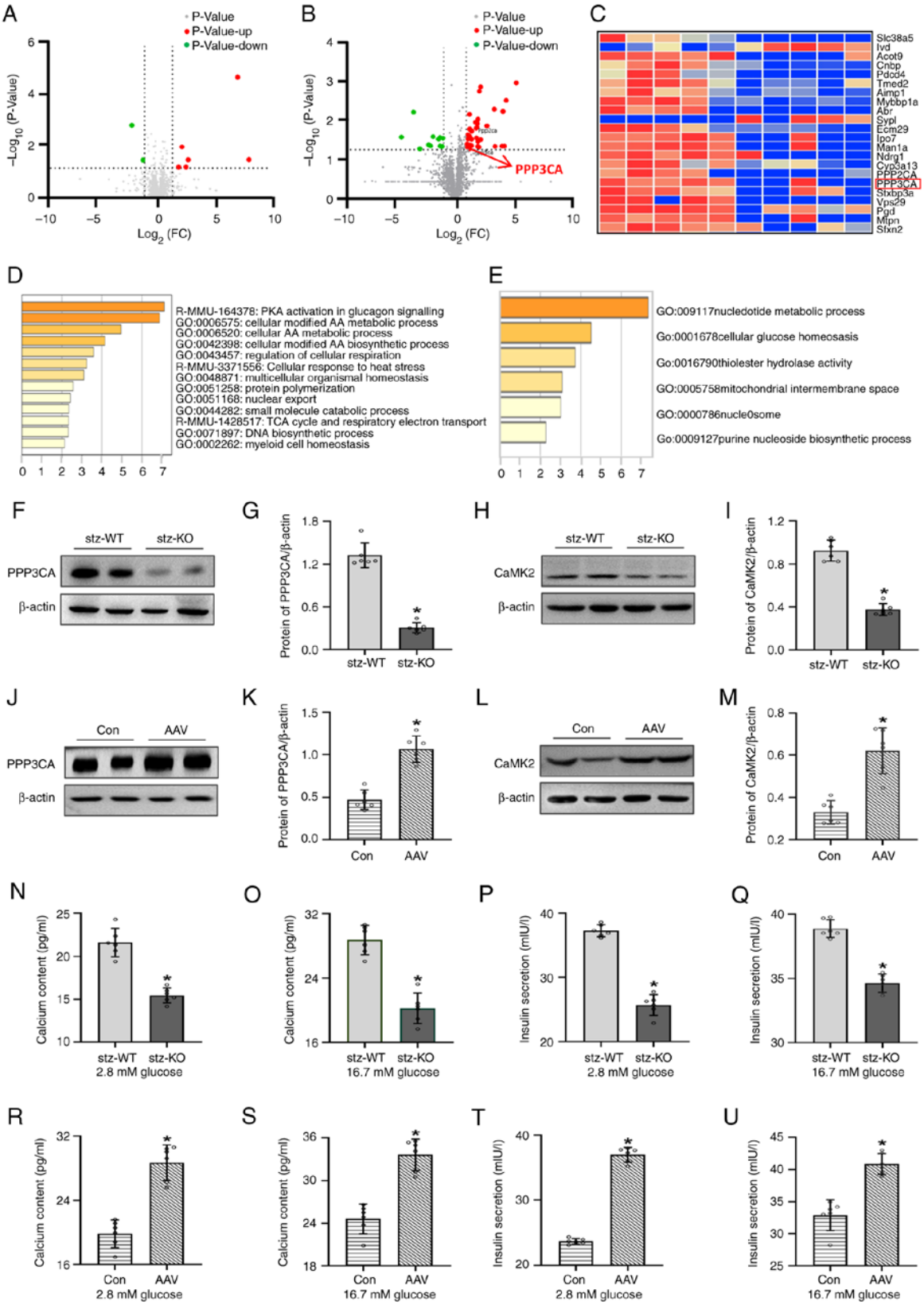

Figure 5. Proteomics analysis and verification of proteins in the Ca^{2+}/CaMK2 pathway in islet β cells. (A) Volcano showed differentially expressed proteins of VEGFB$^{-/-}$ and VEGFB$^{+/+}$ mice in quantitative analysis. (B) Volcano demonstrated differentially expressed proteins of STZ-KO and STZ-WT mice in quantitative analysis, -log10 (P-value) and log2 (Fold change) were used to draw the curve. The upregulated proteins in β cells were colored red, and the downregulated proteins were colored green. (C) The heat map revealed that PPP3CA has an association between VEGFB and differential proteins based on BXD family data. (D) Protein pathway that significantly expresses in VEGFB$^{-/-}$ and VEGFB$^{+/+}$ mice with IPA analysis. (E) Protein pathway that significantly expresses in STZ-KO and STZ-WT mice with IPA analysis. (F-I) Expression of PPP3CA and CaMK2 protein in STZ-KO and STZ-WT mice (n=6). *P<0.05 vs. STZ-WT. (J-M) Expression of PPP3CA and CaMK2 protein in AAV-control and AAV-VEGFB^{186} mice (n=6). *P<0.05 vs. AAV-control. (N-Q) Calcium and insulin contents under the stimulation of 2.8 and 16.7 mmol/l in STZ-KO and STZ-WT mice (n=6). *P<0.05 vs. STZ-WT. (R-U) Calcium and insulin contents under the stimulation of 2.8 and 16.7 mmol/l in AAV-control and AAV-VEGFB^{186} mice (n=6). *P<0.05 vs. AAV-control. VEGFB, vascular endothelial growth factor B; STZ, streptozocin; KO, knockout; WT, wild-type.

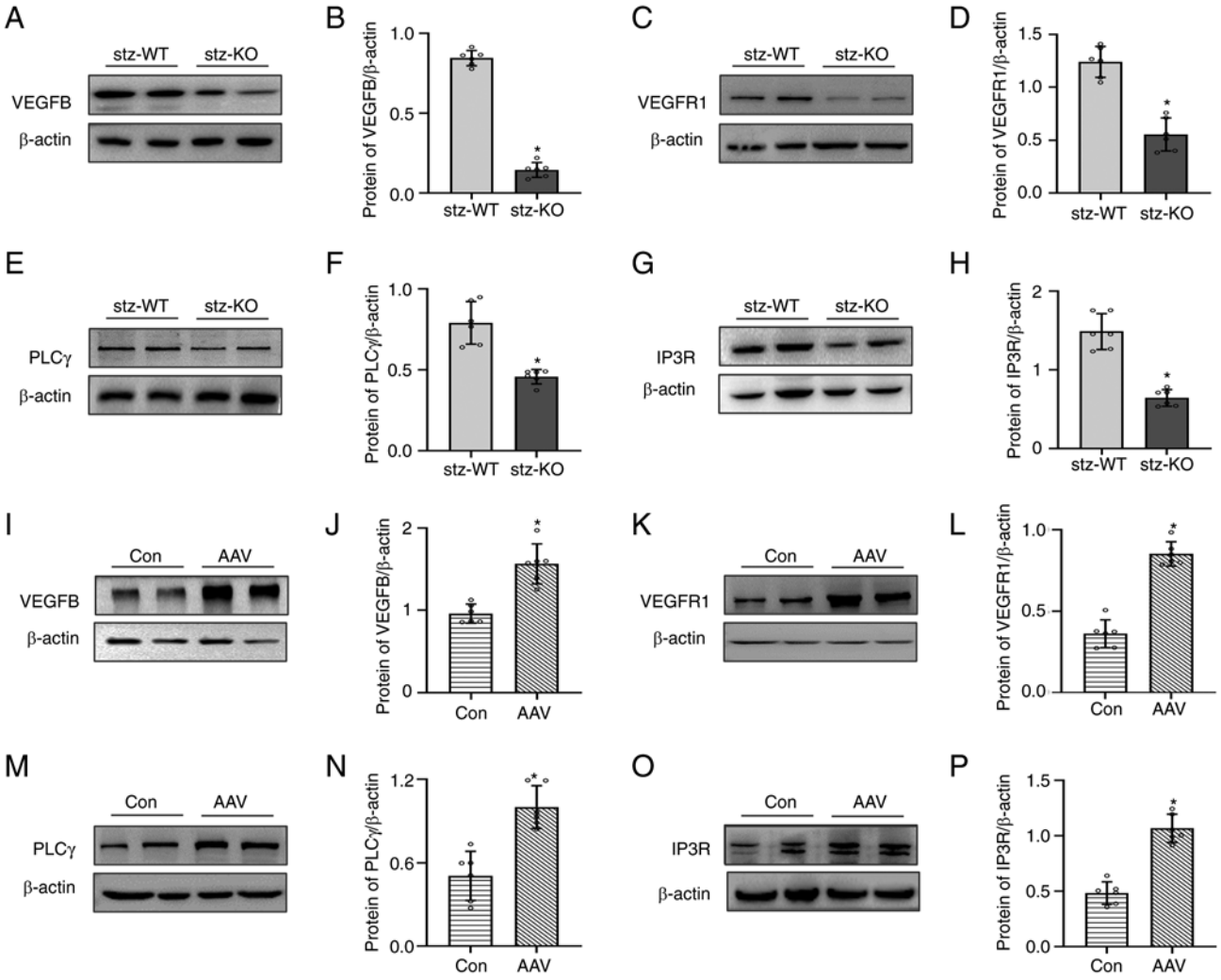

Figure 6. Verification of VEGFB, VEGFR1, PLCγ and IP3R pathway in islet β cells. (A-D) Expression of VEGFB and VEGFR1 proteins of STZ-KO and STZ-WT mice (n=6). (E-H) Expression of PLCγ and IP3R proteins of STZ-KO and STZ-WT mice (n=6). *P<0.05 vs. STZ-WT. (I-L) Expression of VEGFB and VEGFR1 proteins of AAV-control and AAV-VEGFB^{186} mice (n=6). (M-P) Expression of PLCγ and IP3R protein of AAV-control and AAV-VEGFB^{186} mice (n=6). *P<0.05 vs. AAV-control. VEGFB, vascular endothelial growth factor B; STZ, streptozocin; KO, knockout; WT, wild-type; AAV, adeno-associated virus.

VEGFR1 was reduced and the expression levels of VEGFA and VEGFR2 were elevated in the SI group (Fig. S1R-T).

Discussion

VEGFB) is a glycoprotein with high metabolic activity, which has been a late discovery factor in VEGF families (19). However, its role in promoting angiogenesis is not ascertained (19,20). It was previously reported that VEGFB can regulate free fatty acid uptake in endothelial cells by adjusting fatty acid transporters (21). The expression of VEGFB and fatty acid transporters increased after binding with VEGFR1, which resulted in hyperglycemia (22). Paradoxically, a previous study reported that VEGFB suppressed inflammation related to obesity and ameliorated lipid homeostasis since it was transduced into obese mice (23). An increasing number of researchers were interested in deciphering the peculiar regulatory effect of VEGFB on lipid metabolism due to this controversial phenomenon. Numerous studies have identified that VEGFB can inhibit lipid deposition and improve lipid metabolism (24). VEGFB-deficient mice had white fat swelling and increased lipid accumulation. Fat-specific VEGFB inhibition could promote lipid deposition (25). However, the combination of VEGFB and IL22 proteins could reduce lipid deposition by suppressing fatty acid transporters (26). The findings of the present study were similar to the aforementioned studies. T2DM mice gained weight and elevated serum TC and TG after VEGFB KO. VEGFB^{186} overexpression improved lipid metabolism in T2DM mice.

The increase in TG causes ectopic lipid deposition, damages β cell function and affects insulin secretion (27,28). A correlation was found between VEGFB and TC, TG and blood glucose in patients with T2DM. The plasma VEGFB levels in newly diagnosed patients with T2DM was closely related to glucose metabolism and insulin level (3). The VEGFB expression in the renal tissue of patients with diabetic nephropathy was positively correlated with the content of gamma-hydroxybutyric acid (26). The present study illustrated that blood glucose increased after VEGFB KO, as the growth of blood lipids in T2DM mice increased. VEGFB overexpression can

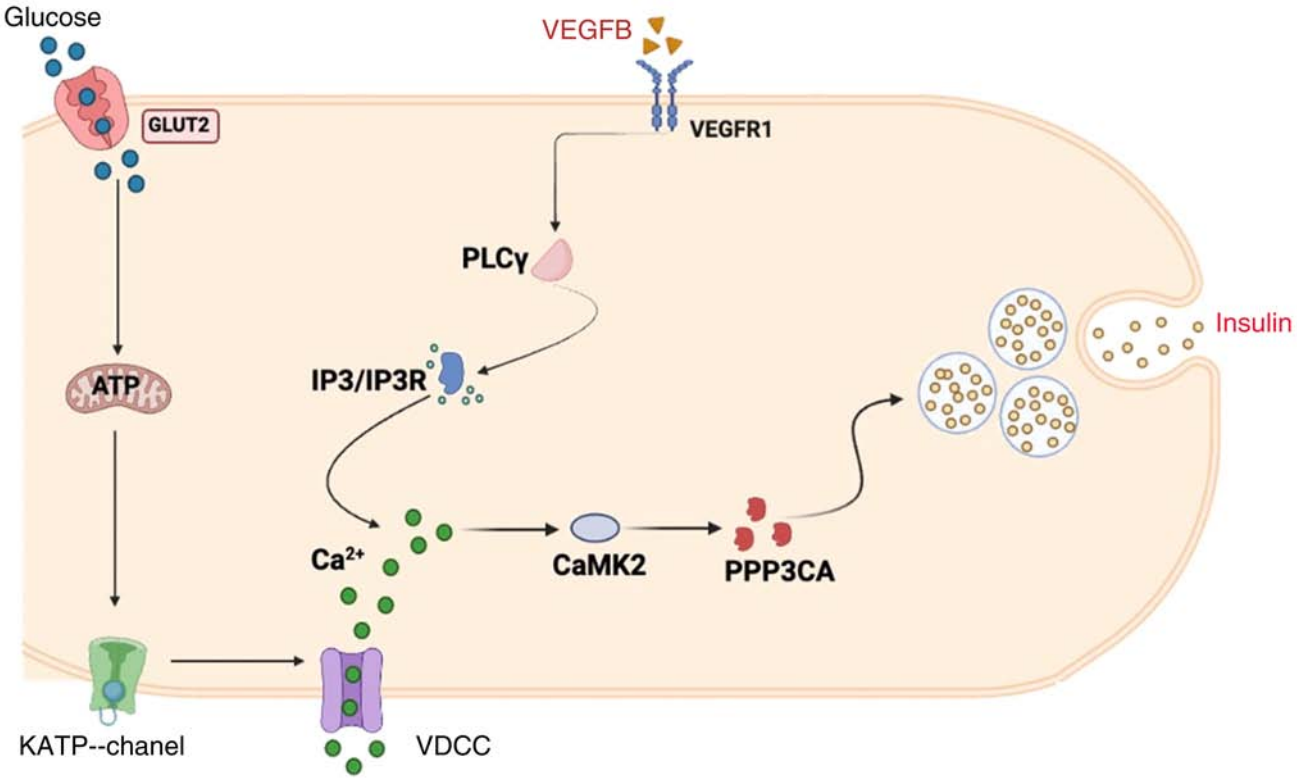

Figure 7. Pattern diagram of VEGFB gene regulating insulin secretion in β cells. VEGFB, vascular endothelial growth factor B.

improve glucolipid metabolism in T2DM mice. The regulatory effect of VEGFB on glucose metabolism may be related to the reduction of TG in T2DM mice.

The markers of T2DM pathogenesis include islet dysfunction and a reduced number of β cells (28). Glucotoxicity damages the β cell and impairs insulin secretion function (29). Decreased β cell function will influence insulin secretion although the number of β cells has a certain impact on T2DM (30). Hyperglycemia will worsen β cell damage, affecting insulin secretion (31). The present study revealed that loss of VEGFB exacerbated β cell population reduction in T2DM mice. However, VEGFB overexpression attenuates β cell injury in T2DM mice. These results of the present study indicated that VEGFB can alleviate β cell damage to insulin secretion. The insulin of T2DM mice decreased after VEGFB KO, and the evaluation index of insulin secretion decreased, indicating that VEGFB has an effect on basic and early insulin secretion function.

Insulin is released from insulin secretory vesicles in pancreatic β cells. Insulin secretory vesicles are divided into immature and mature vesicles (32). Proinsulin is encapsulated into immature insulin secretory vesicles with low electron density and has to undergo through a series of tight regulatory procedures to develop into mature insulin secretory vesicles (33). The mature secretory vesicles are composed of insulin, zinc and calcium crystals, containing dense core vesicles (34). Mature insulin secretory vesicles are stored in the vesicle pool or transported near the cell membrane (35). Insulin secretory vesicles fuse with the cell membrane to release insulin when the blood glucose level increases. The present study revealed that VEGFB can regulate insulin synthesis by affecting the number of immature vesicles in β cells. Concurrently, VEGFB can regulate insulin secretion by affecting the number of mature vesicles.

VEGFR, a specific VEGF receptor, elicits a variety of biological functions through a combination of corresponding VEGF. At present, the VEGFR family contains five members, and VEGFR1, VEGFR2 and VEGFR3 belong to receptor tyrosine kinases (36). The function of VEGFB on lipid homeostasis is strongly dependent on VEGFR1 (37). VEGFB could enhance fatty acid uptake by endothelial cells through VEGFR1 (21). VEGFR1 KO in mice with obesity and insulin resistance could decrease insulin secretion (23). The results of the present study revealed consistent VEGFR1 expression with VEGFB expression after VEGFB KO or overexpression in T2DM mice. Consequently, it was revealed that VEGFB combines with VEGFR1 to regulate insulin secretion in T2DM mice.

The intracellular VEGFR-mediated signal transduction is a complex process. The mechanism of the VEGFR1-mediated signaling pathway is not clear and remains a current research hotspot. The VEGFR1-mediated signaling pathway can activate numerous biological reactions. A previous study revealed that the VEGFR1-mediated signal transduction pathway could activate intracellular MAPK signal transduction by binding with PIGF (38). VEGFR1 suppression could inhibit the expression of its upstream PI3K/AKT signaling pathway (39). VEGFR1 is involved in the PKGI signaling pathway (40). Additionally, the combination of VEGFB and VEGFR1 could activate the intracellular PLCγ signal transduction (41). PLCγ activation produces IP3 (42). PLCγ and IP3 combination could effectively stimulate calcium efflux. PLCγ activation

releases Ca^{2+}, promotes β cell function, and improves insulin secretion to prevent the occurrence of hyperglycemia (43). It was observed in the present study that VEGFB/VEGFR1 could affect Ca^{2+} content in β cells by activating the PLCγ/IP3 signaling pathway to regulate insulin secretion.

Additionally, CaMK is the main mediator of calcium (44). The CaMK expressed in β cells is CaMK2 which is a multifunctional Ca^{2+}/CaMK and is activated by glucose and other insulin secretagogues (45). It has the function of phosphorylating a variety of proteins and is crucial for insulin secretion. Moreover, CaMK2 needs to supplement the reserve vesicle pool in β cells after stimulation is completed (46). The present study is consistent with those revelations, showing that VEGFB can promote Ca^{2+} by activating the CaMK2 to regulate insulin secretion.

PPP3CA was further analyzed and it was found that is associated with VEGFB in differential proteins through proteomics and bioinformatics. In 2008, Wang *et al* reported that PPP3CA modulates the VEGF-stimulated cell proliferation and signaling cascades in cells (47). PPP3CA is a serine/threonine phosphatase regulated by Ca^{2+}/CaM (48,49). Gelernter *et al* found that PPP3CA encodes a calcium-dependent, calmodulin-stimulated protein phosphatase involved in calcium signaling (50). The secretion of Ca^{2+} depends on insulin resistance and type 2 diabetes. Insulin secretion pathways were reported to be activated by upregulating PPP3CA (51,52). PPP3CA can be involved in complications of diabetes (53). Therefore, it was confirmed that PPP3CA and CAMK2 variations are consistent in VEGFB regulation of insulin secretion in T2DM mice, which indicated that VEGFB may stimulate insulin secretion by activating Ca^{2+}/CaM to accelerate substrate protein phosphorylation (Fig. 7).

Moreover, the present study revealed decreased blood glucose and increased insulin secretion in $VEGFB^{-/-}$ mice fed with SD in the 24th week, which was different from the variation in T2DM mice with VEGFB KO. This may be associated with the leverage function of VEGFB in maintaining homeostasis. VEGFB does not play an obvious biological function in a physiological state, while it plays as a safety guard in a pathological state (54-56). Therefore, it was hypothesized that the mechanisms of VEGFB that regulate insulin secretion are different under physiological and pathological conditions. VEGFB may participate in the regulation of insulin secretion through the VEGFA/VEGFR1 signaling pathway under physiological conditions, unlike the regulatory mechanism of VEGFB on insulin secretion in T2DM mice. The signal system of the VEGF family is complex, and the affinity and selectivity of members to different receptors are different. VEGFA can combine with VEGFR1 and VEGFR2, while VEGFB can only combine with VEGFR1 (57,58). The present study supports that VEGFR2 plays a dominant role in all receptors. Some researchers consider that VEGFR1 is a decoy receptor. In general, it not only transmits mitogenic signals but also blocks VEGF, thereby preventing VEGF from binding to VEGFR2. VEGFR1 can negatively regulate the VEGFR2 signaling pathway and promote VEGFR2 under certain pathological conditions (59). At present, the specific mechanism is not completely clear. VEGFR1 expression was downregulated in the present study, while VEGFA and VEGFR2 expression levels were upregulated after the loss of VEGFB in the islets β cell of mice fed with SD. Same results were acquired through the validation of the Min6 cell line. It was indicated that the increase of insulin secretion after VEGFB KO may be related to the VEGFA/VEGFR2 signaling pathway upregulation caused by the decreased VEGFR1 expression under physiological conditions (Fig. S1U). The specific mechanism remains unclear although it was validated in Min6 cells in the present study. In the future, the association between VEGFB and VEGFA/VEGFR2 shall be further validated by the authors using receptor blockers at the *in vivo* and *in vitro* levels.

Acknowledgements

Not applicable.

Funding

The present study was supported by the National Natural Science Foundation of China (grant no. 31771284), the Basic Research Project of Yantai Science and Technology Innovation and Development Plan (grant no. 2022JCYJ026) and the Natural Science Foundation of Shandong province (grant no. ZR202111250163).

Availability of data and materials

The datasets used and/or analyzed during the current study are available from the corresponding author on reasonable request. The mass spectrometry proteomics data have been deposited to the Proteome Xchange Consortium via the PRIDE partner repository with the dataset identifier PXD043843 (https://www.ebi.ac.uk/pride/).

Authors' contributions

YQL, RRL and XL conceptualized and designed experiments, analyzed and interpreted data and drafted the article. FX, MZY, LHZ, QHW, WGJ and YNL designed and conducted experiments, acquired, analyzed and interpreted the data, and revised the article critically for intellectual content. All authors read and approved the final version of the manuscript. WGJ and YNL confirming the authenticity of all the raw data.

Ethics approval and consent to participate

The present study was reviewed and approved by the Institutional Review Board of Binzhou Medical University (Yantai, China). All procedures involving animals were reviewed and approved (IACUC approval no. 2022-210) by the Institutional Animal Care and Use Committee of the Medical Ethics Committee of Binzhou Medical University (Yantai, China).

Patient consent for publication

Not applicable.

Competing interests

The authors declare that they have no competing interests.

References

1. Rorsman P and Braun M: Regulation of insulin secretion in human pancreatic islets. Annu Rev Physiol 75: 155-179, 2013.
2. Cernea S and Dobreanu M: Diabetes and beta cell function: From mechanisms to evaluation and clinical implications. Biochem Med (Zagreb) 23: 266-280, 2013.
3. Wu J, Wei H, Qu H, Feng Z, Long J, Ge Q and Deng H: Plasma vascular endothelial growth factor B levels are increased in patients with newly diagnosed type 2 diabetes mellitus and associated with the first phase of glucose-stimulated insulin secretion function of β-cell. J Endocrinol Invest 40: 1219-1226, 2017.
4. Ning FC, Jensen N, Mi J, Lindström W, Balan M, Muhl L, Eriksson U, Nilsson I and Nyqvist D: VEGF-B ablation in pancreatic beta-cells upregulates insulin expression without affecting glucose homeostasis or islet lipid uptake. Sci Rep 10: 923, 2020.
5. Shang R, Lal N, Lee CS, Zhai Y, Puri K, Seira O, Boushel RC, Sultan I, Räsänen M, Alitalo K, *et al*: Cardiac-specific VEGFB overexpression reduces lipoprotein lipase activity 2 and improves insulin action in rat heart. Am J Physiol Endocrinol Metab 321: E753-E765, 2021.
6. Rorsman P and Ashcroft FM: Pancreatic β-cell electrical activity and insulin secretion: Of mice and men. Physiol Rev 98: 117-214, 2018.
7. Vishnu N, Hamilton A, Bagge A, Wernersson A, Cowan E, Barnard H, Sancak Y, Kamer KJ, Spégel P, Fex M, *et al*: Mitochondrial clearance of calcium facilitated by MICU2 controls insulin secretion. Mol Metab 51: 101239, 2021.
8. Wiederkehr A and Wollheim CB: Minireview: Implication of mitochondria in insulin secretion and action. Endocrinology 147: 2643-2649, 2006.
9. Rask-Madsen C and King GL: Differential regulation of VEGF signaling by PKC-alpha and PKC-epsilon in endothelial cells. Arterioscler Thromb Vasc Biol 28: 919-924, 2008.
10. Chen YH, Chang M and Davidson BL: Molecular signatures of disease brain endothelia provide new sites for CNS-directed enzyme therapy. Nat Med 15: 1215-1218, 2009.
11. Corbett BF, You JC, Zhang X, Pyfer MS, Tosi U, Iascone DM, Petrof I, Hazra A, Fu CH, Stephens GS, *et al*: ΔFosB regulates gene expression and cognitive dysfunction in a mouse model of Alzheimer's Disease. Cell Rep 20: 344-355, 2017.
12. Ding H, Underwood R, Lavalley N and Yacoubian TA: 14-3-3 inhibition promotes dopaminergic neuron loss and 14-3-3theta overexpression promotes recovery in the MPTP mouse model of Parkinson's disease. Neuroscience 307: 73-82, 2015.
13. Liu J, Ibi D, Taniguchi K, Lee J, Herrema H, Akosman B, Mucka P, Hernandez MA, Uyar MF, Park SW, *et al*: Inflammation improves glucose homeostasis through IKKβ-XBP1s interaction. Cell 167: 1052-1066 e1018, 2016.
14. Li X, Wu Y, Zhao J, Wang H, Tan J, Yang M, Li Y, Deng S, Gao S, Li H, *et al*: Distinct cardiac energy metabolism and oxidative stress adaptations between obese and non-obese type 2 diabetes mellitus. Theranostics 10: 2675-2695, 2020.
15. Sun J, Fu X, Liu Y, Wang Y, Huo B, Guo Y, Gao X, Li W and Hu X: Hypoglycemic effect and mechanism of honokiol on type 2 diabetic mice. Drug Des Devel Ther 9: 6327-6342, 2015.
16. Livak KJ and Schmittgen TD: Analysis of relative gene expression data using real-time quantitative PCR and the 2(-Delta Delta C(T)) method. Methods 25: 402-408, 2001.
17. Peterson QP, Veres A, Chen L, Slama MQ, Kenty JHR, Hassoun S, Brown MR, Dou H, Duffy CD, Zhou Q, *et al*: A method for the generation of human stem cell-derived alpha cells. Nat Commun 11: 2241, 2020.
18. Stuhlmann T, Planells-Cases R and Jentsch TJ: LRRC8/VRAC anion channels enhance β-cell glucose sensing and insulin secretion. Nat Commun 9: 1974, 2018.
19. Lal N, Chiu AP, Wang F, Zhang D, Jia J, Wan A, Vlodavsky I, Hussein B and Rodrigues B: Loss of VEGFB and its signaling in the diabetic heart is associated with increased cell death signaling. Am J Physiol Heart Circ Physiol 312: H1163-H1175, 2017.
20. Dmytriyeva O, de Diego Ajenjo A, Lundo K, Hertz H, Rasmussen KK, Christiansen AT, Klingelhofer J, Nielsen AL, Hoeber J, Kozlova E, *et al*: Neurotrophic effects of vascular endothelial growth factor B and novel mimetic peptides on neurons from the central nervous system. ACS Chem Neurosci 11: 1270-1282, 2020.
21. Hagberg CE, Falkevall A, Wang X, Larsson E, Huusko J, Nilsson I, van Meeteren LA, Samen E, Lu L, Vanwildemeersch M, *et al*: Vascular endothelial growth factor B controls endothelial fatty acid uptake. Nature 464: 917-921, 2010.
22. McDonald DM: Tighter lymphatic junctions prevent obesity. Science 361: 551-552, 2018.
23. Robciuc MR, Kivela R, Williams IM, de Boer JF, van Dijk TH, Elamaa H, Tigistu-Sahle F, Molotkov D, Leppänen VM, Käkelä R, *et al*: VEGFB/VEGFR1-induced expansion of adipose vasculature counteracts obesity and related metabolic complications. Cell Metab 23: 712-724, 2016.
24. Zafar MI, Zheng J, Kong W, Ye X, Gou L, Regmi A and Chen LL: The role of vascular endothelial growth factor-B in metabolic homoeostasis: Current evidence. Biosci Rep 37: BSR20171089, 2017.
25. Chen Y, Zhao M, Wang C, Wen H, Zhang Y, Lu M, Adlat S, Zheng T, Zhang M, Li D, *et al*: Adipose vascular endothelial growth factor B is a major regulator of energy metabolism. J Endocrinol 244: 511-521, 2020.
26. Shen Y, Chen W, Han L, Bian Q, Fan J, Cao Z, Jin X, Ding T, Xian Z, Guo Z, *et al*: VEGF-B antibody and interleukin-22 fusion protein ameliorates diabetic nephropathy through inhibiting lipid accumulation and inflammatory responses. Acta Pharm Sin B 11: 127-142, 2021.
27. Su K, Yi B, Yao BQ, Xia T, Yang YF, Zhang ZH and Chen C: Liraglutide attenuates renal tubular ectopic lipid deposition in rats with diabetic nephropathy by inhibiting lipid synthesis and promoting lipolysis. Pharmacol Res 156: 104778, 2020.
28. Herman-Edelstein M, Scherzer P, Tobar A, Levi M and Gafter U: Altered renal lipid metabolism and renal lipid accumulation in human diabetic nephropathy. J Lipid Res 55: 561-572, 2014.
29. Weir GC: Glucolipotoxicity, β-Cells, and diabetes: The emperor has no clothes. Diabetes 69: 273-278, 2020.
30. Campbell JE and Newgard CB: Mechanisms controlling pancreatic islet cell function in insulin secretion. Nat Rev Mol Cell Biol 22: 142-158, 2021.
31. Li M, Abraham NG, Vanella L, Zhang Y, Inaba M, Hosaka N, Hoshino S, Shi M, Ambrosini YM, Gershwin ME, *et al*: Successful modulation of type 2 diabetes in db/db mice with intra-bone marrow-bone marrow transplantation plus concurrent thymic transplantation. J Autoimmun 35: 414-423, 2010.
32. Nasteska D, Fine NHF, Ashford FB, Cuozzo F, Viloria K, Smith G, Dahir A, Dawson PWJ, Lai YC, Bastidas-Ponce A, *et al*: PDX1(LOW) MAFA(LOW) beta-cells contribute to islet function and insulin release. Nat Commun 12: 674, 2021.
33. Liu M, Wright J, Guo H, Xiong Y and Arvan P: Proinsulin entry and transit through the endoplasmic reticulum in pancreatic beta cells. Vitam Horm 95: 35-62, 2014.
34. Slepchenko KG, James CB and Li YV: Inhibitory effect of zinc on glucose-stimulated zinc/insulin secretion in an insulin-secreting beta-cell line. Exp Physiol 98: 1301-1311, 2013.
35. Omar-Hmeadi M and Idevall-Hagren O: Insulin granule biogenesis and exocytosis. Cell Mol Life Sci 78: 1957-1970, 2021.
36. Apte RS, Chen DS and Ferrara N: VEGF in signaling and disease: Beyond discovery and development. Cell 176: 1248-1264, 2019.
37. Hu L, Shan Z, Wang F, Gao X and Tong Y: Vascular endothelial growth factor B exerts lipid-lowering effect by activating AMPK via VEGFR1. Life Sci 276: 119401, 2021.
38. Golfmann K, Meder L, Koker M, Volz C, Borchmann S, Tharun L, Dietlein F, Malchers F, Florin A, Büttner R, *et al*: Synergistic anti-angiogenic treatment effects by dual FGFR1 and VEGFR1 inhibition in FGFR1-amplified breast cancer. Oncogene 37: 5682-5693, 2018.
39. Ling M, Quan L, Lai X, Lang L, Li F, Yang X, Fu Y, Feng S, Yi X, Zhu C, *et al*: VEGFB promotes myoblasts proliferation and differentiation through VEGFR1-PI3K/Akt signaling pathway. Int J Mol Sci 22: 13352, 2021.
40. Shen Z, Zhang Z, Wang X and Yang K: VEGFB-VEGFR1 ameliorates Ang II-induced cardiomyocyte hypertrophy through Ca(2+)-mediated PKG I pathway. J Cell Biochem 119: 1511-1520, 2018.
41. Weddell JC, Chen S and Imoukhuede PI: VEGFR1 promotes cell migration and proliferation through PLCgamma and PI3K pathways. NPJ Syst Biol Appl 4: 1, 2018.
42. Kadamur G and Ross EM: Mammalian phospholipase C. Annu Rev Physiol 75: 127-154, 2013.
43. Liang S, Zhao J, Wang Q, Yang M, Wang X, Chen S, Chen M and Sun C: Carbon monoxide enhances calcium transients and glucose-stimulated insulin secretion from pancreatic β-cells by activating Phospholipase C signal pathway in diabetic mice. Biochem Biophys Res Commun 582: 1-7, 2021.

44. Takemoto-Kimura S, Suzuki K, Horigane SI, Kamijo S, Inoue M, Sakamoto M, Fujii H and Bito H: Calmodulin kinases: Essential regulators in health and disease. J Neurochem 141: 808-818, 2017.
45. Choi SE, Shin HC, Kim HE, Lee SJ, Jang HJ, Lee KW and Kang Y: Involvement of Ca2+, CaMK II and PKA in EGb 761-induced insulin secretion in INS-1 cells. J Ethnopharmacol 110: 49-55, 2007.
46. Miyano R, Miki T and Sakaba T: Ca-dependence of synaptic vesicle exocytosis and endocytosis at the hippocampal mossy fibre terminal. J Physiol 597: 4373-4386, 2019.
47. Wang K, Song Y, Chen DB and Zheng J: Protein phosphatase 3 differentially modulates vascular endothelial growth factor- and fibroblast growth factor 2-stimulated cell proliferation and signaling in ovine fetoplacental artery endothelial cells. Biol Reprod 79: 704-710, 2008.
48. Panneerselvam S, Wang J, Zhu W, Dai H, Pappas JG, Rabin R, Low KJ, Rosenfeld JA, Emrick L, Xiao R, *et al*: PPP3CA truncating variants clustered in the regulatory domain cause early-onset refractory epilepsy. Clin Genet 100: 227-233, 2021.
49. Wu J, Zheng C, Wang X, Yun S, Zhao Y, Liu L, Lu Y, Ye Y, Zhu X, Zhang C, *et al*: MicroRNA-30 family members regulate calcium/calcineurin signaling in podocytes. J Clin Invest 125: 4091-4106, 2015.
50. Gelernter J, Kranzler HR, Sherva R, Koesterer R, Almasy L, Zhao H and Farrer LA: Genome-wide association study of opioid dependence: Multiple associations mapped to calcium and potassium pathways. Biol Psychiatry 76: 66-74, 2014.
51. Fong CC, Wei F, Chen Y, Yu WK, Koon CM, Leung PC, Fung KP, Lau CB and Yang M: Danshen-gegen decoction exerts proliferative effect on rat cardiac myoblasts H9c2 via MAPK and insulin pathways. J Ethnopharmacol 138: 60-66, 2011.
52. Zhao Y, Xue Q, Su X, Xie L, Yan Y, Wang L and Steinman AD: First identification of the toxicity of microcystins on pancreatic islet function in humans and the involved potential biomarkers. Environ Sci Technol 50: 3137-3144, 2016.
53. Atkin AS, Moin ASM, Nandakumar M, Al-Qaissi A, Sathyapalan T, Atkin SL and Butler AE: Impact of severe hypoglycemia on the heat shock and related protein response. Sci Rep 11: 17057, 2021.
54. Li X, Kumar A, Zhang F, Lee C and Tang Z: Complicated life, complicated VEGF-B. Trends Mol Med 18: 119-127, 2012.
55. Gao R, Zhu BH, Tang SB, Wang JF and Ren J: Scutellarein inhibits hypoxia- and moderately-high glucose-induced proliferation and VEGF expression in human retinal endothelial cells. Acta Pharmacol Sin 29: 707-712, 2008.
56. Koch S, Tugues S, Li X, Gualandi L and Claesson-Welsh L: Signal transduction by vascular endothelial growth factor receptors. Biochem J 437: 169-183, 2011.
57. Anisimov A, Leppanen VM, Tvorogov D, Zarkada G, Jeltsch M, Holopainen T, Kaijalainen S and Alitalo K: The basis for the distinct biological activities of vascular endothelial growth factor receptor-1 ligands. Sci Signal 6: ra52, 2013.
58. Uemura A, Fruttiger M, D'Amore PA, De Falco S, Joussen AM, Sennlaub F, Brunck LR, Johnson KT, Lambrou GN, Rittenhouse KD and Langmann T: VEGFR1 signaling in retinal angiogenesis and microinflammation. Prog Retin Eye Res 84: 100954, 2021.
59. Cudmore MJ, Hewett PW, Ahmad S, Wang KQ, Cai M, Al-Ani B, Fujisawa T, Ma B, Sissaoui S, Ramma W, *et al*: The role of heterodimerization between VEGFR-1 and VEGFR-2 in the regulation of endothelial cell homeostasis. Nat Commun 3: 972, 2012.